Adair-Based Hemoglobin Equilibrium with Oxygen, Carbon Dioxide and Hydrogen Ion Activity*

Marek Mateják, Tomáš Kulhánek, Stanislav Matoušek
From the Institute of Pathological Physiology
First Faculty of Medicine
Charles University in Prague, Czech Republic

*Running title: **Adair-based Hb-O_2-pH-CO_2 equilibrium**

Corresponding author: Marek Matejak, U Nemocnice 5, Prague 2, 128 53, Czech Republic, Tel: +420 776 301 395, Fax: +420 224 965 916, E-mail: marek.matejak@lf1.cuni.cz

ABSTRACT

As has been known for over a century, oxygen binding onto hemoglobin is influenced by the activity of hydrogen ions (H^+), as well as the concentration of carbon dioxide (CO_2). As is also known, the binding of both CO_2 and H^+ on terminal valine-1 residues is competitive. One-parametric situations of these hemoglobin equilibria at specific levels of H^+, O_2 or CO_2 are also well described. However, we think interpolating or extrapolating this knowledge into an "empirical" function of three independent variables has not yet been completely satisfactory. **W**e present a model that integrates three orthogonal views of hemoglobin oxygenation, titration, and carbamination at different temperatures. The model is based only on chemical principles, Adair's oxygenation steps and Van't Hoff equation of temperature dependences. Our model fits the measurements of the Haldane coefficient and CO_2 hemoglobin saturation. It also fits the oxygen dissociation curve influenced by simultaneous changes in H^+, CO_2 and O_2, which makes it a strong candidate for integration into more complex models of blood acid-base with gas transport, where any combination of mentioned substances can appear.

Keywords: Acid-Base Equilibrium; Blood Gas Analysis; Carboxyhemoglobin; Hemoglobin A; Oxyhemoglobins

INTRODUCTION

Human hemoglobin A is one of the most extensively studied protein macromolecules. The composition and 3D conformation of both α and β chains is known [1, 2] and the binding of O_2, H^+ and 2,3-DPG has been described [2, 3]. Since the 1930s it has generally been believed that CO_2 binding to Hb occurs by carbamination of the amino-terminus, forming a carboxylate compound [4-6]. This hemoglobin carbamination was verified by Morrow et al. [7], who used nuclear magnetic resonance of $^{13}CO_2$ to find its exact binding sites at valine-1. The shift of titration between oxygenated and deoxygenated forms is also well known. Called the Bohr or Haldane effect [8-10], it is caused by the same valine-1 side and by more than ten other acid-base residues [2, 11].

The most common descriptions of the hemoglobin oxygen dissociation curve (ODC) are the allosteric models [12, 13], the model based on Hill equation [14, 15], and Adair's four-step model [16]. Some of the ODC models [15, 17, 18] also include the effects of varying pH and CO_2 concentration. However, these models operate only with interpolation or extrapolation of ODC from normal pH or normal pCO_2 and do not take into account the chemical dependences between titration [8] and carbamination [19]. They fail when both pH and CO_2 are not at normal values, especially in the alkaline pH range.

Based on these findings, we propose a hemoglobin binding equilibrium model that starts with a description of hemoglobin-oxygen dissociation using a slightly modified version of Adair's approach [16]. We continue by describing the relationship between CO_2 and H^+ as competitive inhibition in the amino group of terminal valine-1 residue on each chain (suffixes *z* and *c*), which is in accordance with the known facts [4, 6, 20]. Finally, we lump all other acid-base side chains residues in a hemoglobin subunit into one Bohr proton-binding site of the side chain residues. These are denoted by the suffix *h* in the article.

METHODS

The model is built in Mathematica 9.0 (Wolfram, Champaign, IL) and also in Dymola FD01 2014 (Dassault Systemes, Paris, France) as an example of chemical package in open-source Modelica library Physiolibrary 2.2.0 [21, 22] according to the model structure defined in the following section. The model contains only physiological parameters such as gas solubilities and dissociation coefficients of defined reactions. The unknown parameters are fitted to the data of Siggaard-Andersen [23], Bauer and Schröder [24], Severinghaus [18], Matthew et al. [1] and Reeves [25] using Mathematica function FindFit and also using parameter estimation method suggested by Kulhanek et al. [26].

Free dissolved concentrations of $[O_2]$ and $[CO_2]$ in red blood cells are calculated from gas partial pressures using Henry's law ($[O_2]=\alpha O_2 * pO_2$ and $[CO_2]=\alpha CO_2 * pCO_2$) with solubility coefficients $\alpha O_2=1.005*10^{-5}$ $mol.m^{-3}.Pa^{-1}$ measured at 38 °C by Sendroy et al. [27], and $\alpha CO_2=2.3*10^{-4}$ $mol.m^{-3}.Pa^{-1}$ at 37 °C, as proposed by Maas et al. [28]. These solubilities are slightly different from solubilities in pure water or in plasma because of the effects of salts and proteins inside erythrocyte [27].

MODEL STRUCTURE

The model is built upon several simplifying assumptions. Firstly, each of four hemoglobin tetramer subunits is treated as identical, even though (slight) differences are known to exist between α and β subunits. Secondly, CO_2 or H^+ binding is supposed not to affect the CO_2 or H^+ affinities in the other three subunits. Thus, the interaction between the subunits is modeled purely

through the varying affinities of oxygen in each oxygenation step. The third simplifying assumption has already been mentioned; it is lumping all Bohr proton binding sites of subunit into two (first for the valine-1 amino-terminus and second for the side chains residues), a simplification first suggested by Antonini [29].

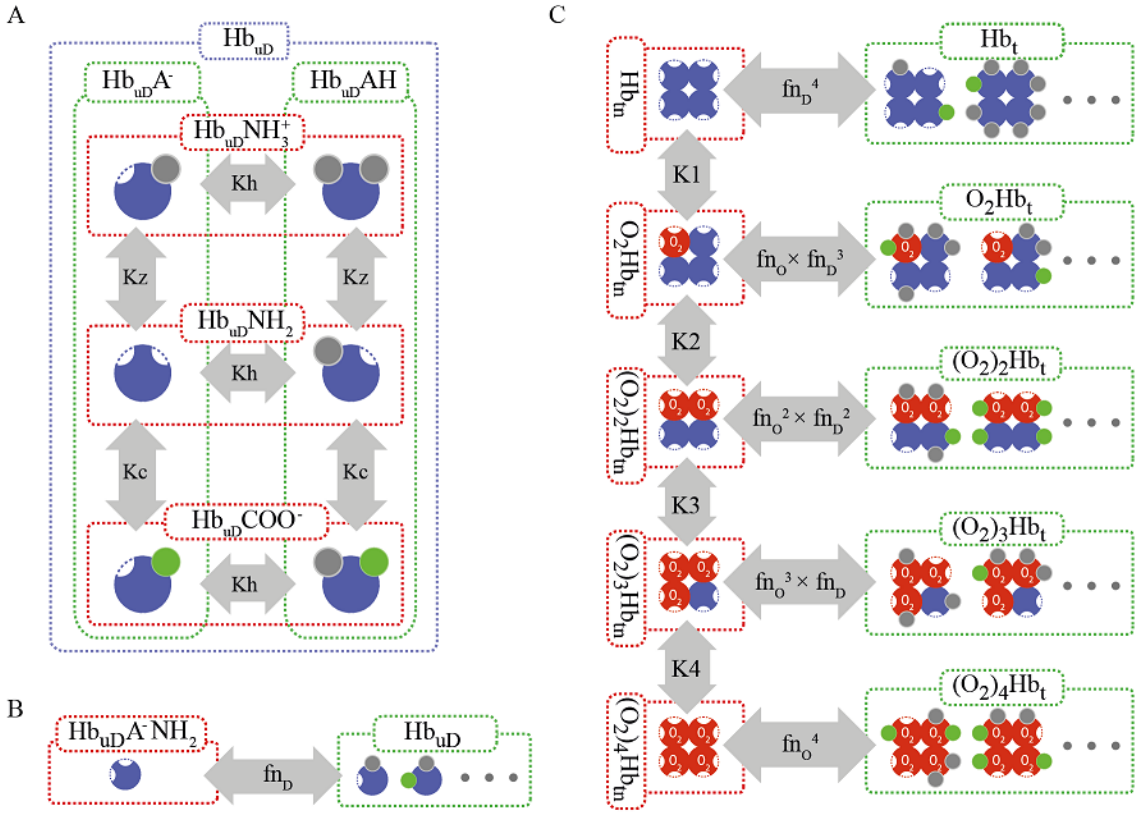

Figure 1, Schema of hemoglobin calculation

A) Possible forms of deoxyhemoglobin subunit (the blue circles). The gray circles represent hydrogen ions, and the green circles represent carbon dioxide. The arrows with dissociation coefficients represent the reactions z, c and h. B) Schema of chemical speciation of deoxyhemoglobin subunit. C) Schema of chemical speciation and Adair's oxygenation steps of hemoglobin tetramer.

Model structure of hemoglobin subunit

The three reactions that participate in the Bohr and Haldane effect of each subunit are as follows:

Reaction z:	$Hb_uNH_3^+$	↔	Hb_uNH_2	+	H^+
Reaction c:	$Hb_uNH_2 + CO_2$	↔	Hb_uCOO^-	+	H^+
Reaction h:	Hb_uAH	↔	Hb_uA^-	+	H^+

where the reactions z and c are competitive on the valine-1 amino-terminus, and the reaction h is independent of z or c.

The chemical equilibrium equations of these three reactions are Eq.1-3, where K_x is the equilibrium dissociation coefficients of the reaction *x* (i.e., *z*, *c* or *h*).

Reaction z: $$K_z = \frac{[Hb_uNH_2] * aH^+}{[Hb_uNH_3^+]} \quad \textbf{(1)}$$

Reaction c: $$K_c = \frac{[Hb_uCOO^-] * aH^+}{[CO_2][Hb_uNH_2]} \quad \textbf{(2)}$$

Reaction h: $$K_h = \frac{[Hb_uA^-] * aH^+}{[Hb_uAH]} \quad \textbf{(3)}$$

These dissociation coefficients are different between oxy and deoxy subunits, which are distinguished by the subscripts O and D in the following text. They can be also written in their logarithmic form, where $\mathbf{pK_x}$ means $-\log_{10}(K_x)$. Thus, for instance, pK_{zO} denotes the equilibrium coefficient of the reaction z for the oxy form of the hemoglobin subunit. Similar notation is used for describing the activity of hydrogen ions (acidity), where $pH=-\log_{10}(aH^+)$.

Using Eq.1-3 it is possible to express fractions for deoxy and oxy subunits. We label these fractions as follows: Hb_uNH_2 fractions are called $\mathbf{f_{zcD}}$ ($\mathbf{f_{zcO}}$), Hb_uA^- fractions $\mathbf{f_{hD}}$ ($\mathbf{f_{hO}}$), $Hb_uA^-NH_2$ fractions $\mathbf{fn_D}$ ($\mathbf{fn_O}$) and Hb_uCOO^- fractions $\mathbf{sCO_{2D}}$ ($\mathbf{sCO_{2O}}$) as in Eq. 4-7. The selection of form $Hb_uA^-NH_2$ from the division into Hb_uNH_2 and Hb_uA^- is also illustrated in Fig. 1A, B.

$$f_{\mathrm{zcD}} = \frac{[Hb_{uD}NH_2]}{[Hb_{uD}]} = \frac{1}{1 + 10^{\mathrm{pKzD}-pH} + [CO_2]10^{pH-pKcD}} \quad \textbf{(4)}$$

$$f_{\mathrm{hD}} = \frac{[Hb_{uD}A^-]}{[Hb_{uD}]} = \frac{1}{10^{\mathrm{pKhD}-pH} + 1} \quad \textbf{(5)}$$

$$fn_{\mathrm{D}} = \frac{[Hb_{uD}A^-NH_2]}{[Hb_{uD}]} = f_{\mathrm{zcD}} \times f_{\mathrm{hD}} \quad \textbf{(6)}$$

$$\mathrm{sCO_{2D}} = \frac{[Hb_{uD}COO^-]}{[Hb_{uD}]} = 10^{pH-pKcD} f_{\mathrm{zcD}}[CO_2] \quad \textbf{(7)}$$

We define a titration shift as the amount of acid that must be added to achieve the same pH after full deoxygenation of the hemoglobin subunit. This change of subunit charge during deoxygenation (by the Bohr protons) is also called Haldane coefficient ΔH^+. The coefficient can be divided into contributions of the previously mentioned reactions ΔH_h^+, ΔH_z^+ and ΔH_c^+, as is algebraically expressed by Eq. 8-11.

$$\Delta H_h^+ = -\frac{[Hb_{uD}A^-] - [Hb_{uO}A^-]}{[Hb_u]} = -(f_{\mathrm{hD}} - f_{\mathrm{hO}}) \quad \textbf{(8)}$$

$$\Delta H_z^+ = \frac{[Hb_{uD}NH_3^+] - [Hb_{uO}NH_3^+]}{[Hb_u]} = \left(\frac{10^{\mathrm{pKzD}}}{10^{pH}} f_{\mathrm{zcD}} - \frac{10^{\mathrm{pKzO}}}{10^{pH}} f_{\mathrm{zcO}}\right) \quad \textbf{(9)}$$

$$\Delta H_c^+ = -\frac{[Hb_{uD}COO^-] - [Hb_{uO}COO^-]}{[Hb_u]} = -(\mathrm{sCO_{2D}} - \mathrm{sCO_{2O}}) \quad \textbf{(10)}$$

$$\Delta H^+ = \Delta H_z^+ + \Delta H_c^+ + \Delta H_h^+ \quad \textbf{(11)}$$

Model structure of hemoglobin tetramer

The speciation of the hemoglobin tetramer molecule can be considered at various levels of detail; the one chosen as appropriate in our approach is indicated in Fig. 1C. The possible forms include different combinations of oxygenated and deoxygenated hemes, protonated and deprotonated oxygen-linked acid groups, and free or carboxylated amino endings of each chain. Yet because of the law of detailed balance in equilibrium [30], it is not necessary to calculate all reactions between these forms. As a result, only four oxygenation reactions need be selected for the calculation. This is done in accordance with Fig. 1C, by selecting a tetramer form $(O_2)_iHb_{tn}$ composed only of four subunits in the form $Hb_uA^-NH_2$ (H^+ and CO_2 free), and modeling oxygen binding to these forms with Adair-type coefficients of the following reactions:

$$\begin{aligned}
O_2Hb_{tn} &\leftrightarrow Hb_{tn} + O_2\\
(O_2)_2Hb_{tn} &\leftrightarrow O_2Hb_{tn} + O_2\\
(O_2)_3Hb_{tn} &\leftrightarrow (O_2)_2Hb_{tn} + O_2\\
(O_2)_4Hb_{tn} &\leftrightarrow (O_2)_3Hb_{tn} + O_2
\end{aligned}$$

where dissociation coefficients are defined by Eq.12, which are also represented by vertical arrows at Fig. 1C.

$$K_\mathrm{i} = \frac{[(O_2)_{i-1}Hb_\mathrm{tn}] \cdot [O_2]}{[(O_2)_iHb_\mathrm{tn}]} \quad \textbf{(12)}$$

For the next calculation, all forms can be expressed as a fraction of the deoxy-tetramer form $(O_2)_0Hb_{tn}$, as shown in Eq. 13.

$$[(O_2)_iHb_\mathrm{tn}] = \frac{[(O_2)_0Hb_{tn}] \cdot [O_2]^i}{\prod_{\mathrm{j}=1}^{\mathrm{i}} \mathrm{K_i}} \quad \textbf{(13)}$$

Let us move the attention from specific forms of Hb_{tn} to the description of the equilibrium within the whole group of Hbt. Looking at Fig. 1C, one can see that for each oxygenation step we can calculate the equilibrium in each horizontal line using Eq. 14.

$$[(O_2)_iHb_\mathrm{t}] \cdot {fn_\mathrm{D}}^{4-i} \cdot {fn_\mathrm{O}}^{i} = [(O_2)_iHb_\mathrm{tn}] \quad \textbf{(14)}$$

The CO_2- and pH-dependent oxygen saturation equation in the Adair style (Eq. 15) is algebraically derived from Eq. 13-14, where $a_\mathrm{i} = 1/(\prod_{\mathrm{j}=1}^{\mathrm{i}} \mathrm{K_j})$ and $x = (\mathrm{fn_D}(pH, [CO_2])/\mathrm{fn_O}(pH, [CO_2])) * [\mathrm{O_2}]$.

$$sO_2 = \frac{a_1\,x\, + 2\,a_2\,x^2 + 3\,a_3\,x^3 + 4\,a_4\,x^4}{4 + 4\,a_1\,x\, + 4\,a_2\,x^2 + 4\,a_3\,x^3 + 4\,a_4\,x^4} \quad \textbf{(15)}$$

Hemoglobin saturation with CO_2 (sCO_2) is calculated separately in oxygenated and deoxygenated subunits forms (sCO_{2O} and sCO_{2D}) using Eq. 16.

$$sCO_2 = sO_2 \cdot sCO_{2O} + (1 - sO_2) \cdot sCO_{2D} \quad \textbf{(16)}$$

Finally, the shift of titration after deoxygenation and decarbamination of the hemoglobin subunit can be expressed by Eq. 17.

$$dTH = sO_2 \cdot \Delta H^+ + sCO_{2D} + \frac{sCO_{2D}}{1 + 10^{pH - pKzD}} \quad \textbf{(17)}$$

Temperature dependences

The temperature dependences are integrated using the Van't Hoff equation (Eq. 18), where R=8.314 $J.K^{-1}.mol^{-1}$ is gas constant, ΔH^{θ} is the standard enthalpy change as an amount of heat consumed by a reaction changing one mole of substrates to products, and K2 and K1 are Henry's coefficients of solution or the dissociation coefficient of the chemical reaction at temperature T2 and T1 (expressed in Kelvin).

$$\ln\left(\frac{K_2}{K_1}\right) = \frac{-\Delta H^{\theta}}{R}\left(\frac{1}{T_2} - \frac{1}{T_1}\right) \quad \textbf{(18)}$$

RESULTS

The Adair's coefficients are fitted to the collection of ODC measurements by Severinghaus [18] at pCO_2=0 Pa and pH_p=7.4, see Fig. 2A and Table I. The dissociation coefficients of carboxylation are determined in close agreement with Bauer and Schröder using their data [24]; the resulting fit can be seen in Fig. 2B, the coefficients are in Table II. The lumped acid dissociation coefficients for the side-chains pKhD and pKhO are estimated by optimization of Siggaard-Andersen's data [23] at DPG/Hbt=0.84, pH=6.5 to 8.0 and 37°C; the resulting fit can be seen in Fig. 2C, and the coefficients complete Table II.

Table I

Estimated form-specific Adair's coefficients [$mol.m^{-3}$] at 37°C			
K_1	K_2	K_3	K_4
0.0121	0.0117	0.0871	0.000386

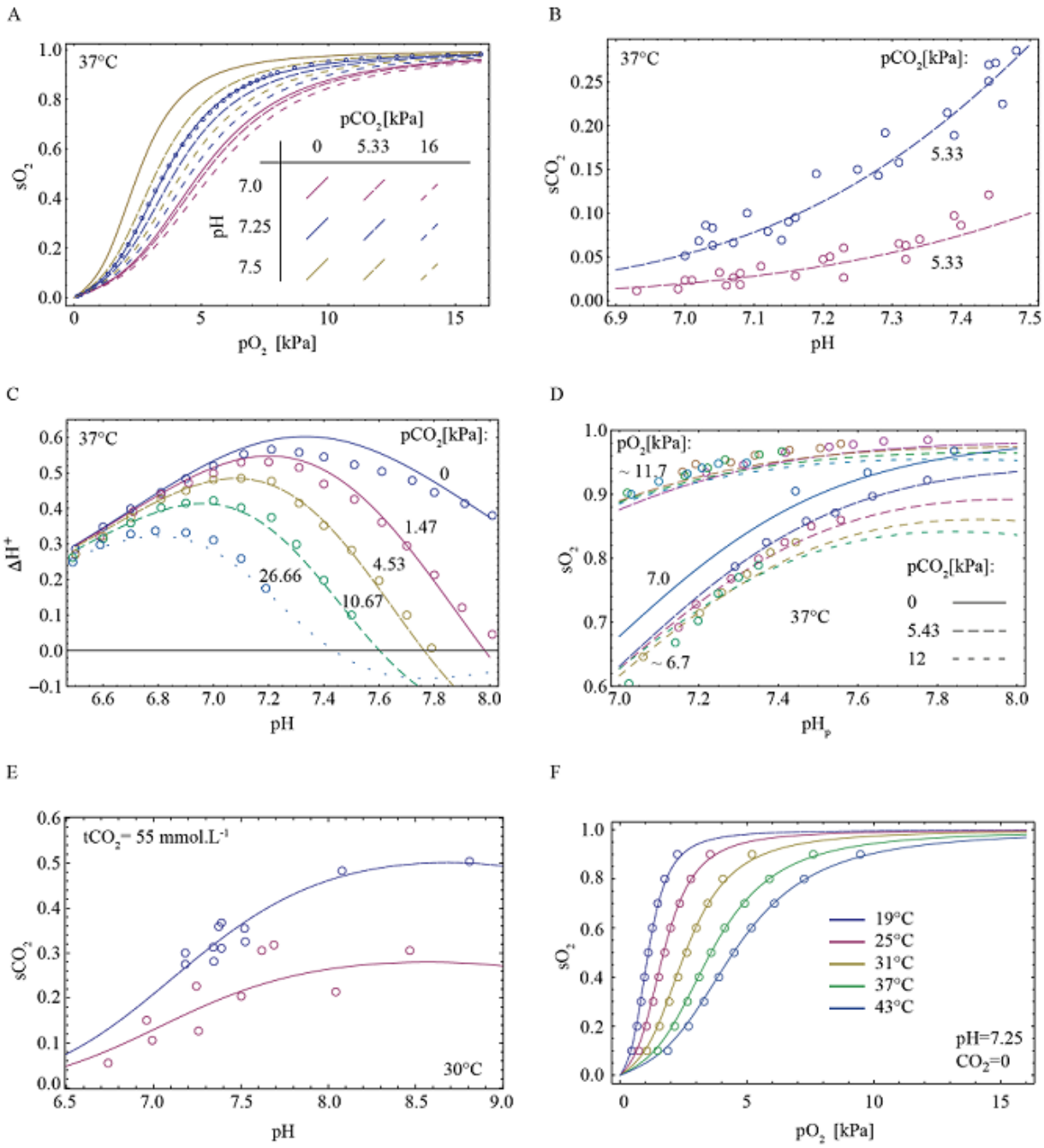

Figure 2, Model curves and measured data points

A) Points are from Severinghaus's oxygen dissociation curve collection [18] at pCO_2=0 Pa, erythrocyte intracellular pH=7.2 and temperature 37°C. Lines are sO_2 defined by Eq. 15 B) Carboxylation of hemoglobin measured and estimated by Bauer and Schröder [24]. The lines (Eq. 7) are sCO_2D and sCO_2O at pCO_2=5.33 kPa.C) Bohr protons released during oxygenation of one hemoglobin subunit. Dots are data measured by Siggaard-Andersen [23] in erythrolysate at 37°C, DPG/Hbt = 0.84. Lines are calculated from Eq. 11 using data from Table II. From top to bottom data are plotted for different pCO_2=0 kPa, 1.47 kPa, 4.53 kPa, 10.67 kPa and 26.66 kPa. D) Naeraa et al.'s [29] oxygen saturation data comparison. The two groups of lines (Eq. 15) are determined mainly by pO_2 around 6.7 kPa and 11.7 kPa. The small nuances in each group are caused by different pCO_2 changed from 0 kPa to 12 kPa. E) Matthew et al.'s [1] carbamination data measured at 30°C with constant content of all carbonates 55 mmol.L-1 . Fitted dissociation constants, which determine the lines, are used to estimate enthalpies of their reactions to be consistent with Bauer and Schröder [24]. F) Reeves [32] oxygen saturation data at different temperatures. Enthalpies of reaction h and specific Adair oxygenation step enthalpy is estimated (lines) to fit the data (circles).

We concluded that the model also describes the ODC shifts by comparing with Naerea et al.'s [31] oxygen saturation measurements at different plasma pH and CO_2 levels, see Fig. 2D. The recalculation of data from plasma pH_p to intracellular erythrocyte pH uses the equation $pH=7.2464+0.796(pH_p-7.4)$, as presented by Siggaard-Andersen and Salling [32].

Table II

Estimated acid dissociation coefficients at 37°C		
reaction z	*reaction c*	*reaction h*
$pK_{zD}=7.73$	$pK_{cD}=4.54$	$pK_{hD}=7.52$
$pK_{zO}=7.25$	$pK_{cO}=5.35$	$pK_{hO}=6.89$

The gas solubility as Henry's coefficient at different temperatures can be recalculated using the enthalpy of gas solution (-14 $kJ.mol^{-1}$ for O_2, and -20 $kJ.mol^{-1}$ for CO_2 [33]). If we assume that the examined hemoglobin of Matthew [1] is at compatible conditions, but at a temperature of 30°C with $pK_{zD}=7.53$, $pK_{zO}=7.28$, $pK_{cD}=4.77$ and $pK_{cO}=5.20$ as plotted in Fig. 2E, then the enthalpies of these reactions are -51, 8, 59 and -41 $kJ.mol^{-1}$. The heat of oxygenation unaffected by oxygen heat of solution, by carbon dioxide and by Bohr protons was measured by Atha and Ackers [34] as 59 $kJ.mol^{-1}$. Using this value for each Adair oxygenation step it is possible to optimize other enthalpies to fit the Reeves data [25], measured at 19-43°C. Resulting as the enthalpies 59 $kJ.mol^{-1}$ of deoxy and -127 $kJ.mol^{-1}$ of oxy version of reaction *h* to reach ODCs curves plotted in Fig. 2F.

DISCUSSION

Having a precise quantitative description of hemoglobin behavior is a crucial aspect in describing the behavior of whole blood, which has numerous uses in medicine today. It is important in areas such as blood gas analysis [15, 35], the building of complex models [36], simulation for teaching purposes [37], or rebreathing-based methods for cardiac output estimation, which represent a more specific use [38]. For instance, the precision of the latter methods is crucially dependent on the exact calculation of the total amount of carbon dioxide in blood for various (abnormal) patient conditions, as has been recently pointed out [39].

This model offers a precise description of various phenomena that take place with hemoglobin, based on relatively simple starting points, such as competitive binding of H+ and CO_2 at valine-1 amino terminus or the law of detailed balance [30]. Even with a simple structure, it offers a remarkably good fit to the data of hemoglobin oxygenation, titration, and carbamination at different temperatures, as shown in Fig. 2A-E. These can be calculated with any combination of oxygen, carbon dioxide and hydrogen ions defined as open system (lungs), where the partial pressures are equilibrated, and also in a closed system (tissues), where mass conservation laws and the total amount of substances take place, as was also modeled by Rees and Andreassen [40], among others.

The results of our model (Fig. 2A-E) show strong nonlinear dependences between variables, which is in agreement with the known data [1, 23-25, 41]. Looking at Fig. A, one can compare sets of ODCs, where each color represents a different pH. Various curves of each color represent

ODCs for various levels of pCO_2 for a given pH. As can be seen, the effect of pCO_2 on the ODC is stronger at high (alkaline) pH, which is in agreement with the data [23]. Similarly, one can compare the curves within the sets of solid or dashed lines, where each set represents dissociation curves for various values of pH at a given level of pCO_2. The variation between the curves of each line type represents the Bohr effect for the given level of CO_2, this effect can also be appreciated from data of Fig. 2C, which shows the average amount of released H^+ upon oxygenation of one hemoglobin subunit.

The model uses enthalpies to calculate temperature dependences of hemoglobin behavior (Fig. 2F,E), which allows examination of the heat transfers during single chemical processes. For instance, binding of aqueous oxygen onto hemoglobin produces 30-40 kJ/mol of heat [42-45], and the same amount of heat is consumed by deoxygenation process in metabolically active tissues, thus helping to cool them down. When the hemoglobin model is used in the standard conditions of a large-scale HumMod model [36], the resulting heat transfer due to the exothermy of the hemoglobin oxygen reaction is 4-7% of the total heat produced by muscle, which is in agreement with experimental results [42, 44, 45]. It is interesting to note that this heat transfer occurs without any increase in blood temperature.

The integration of chemical processes in a macromolecule requires a precise view into their underlying principles. Some physiologists use the elementary chemical equations [40], but do not implement the principle of detailed balance [30]. Other physiologists make empirically-based equations with a raw linear gradient approximation of possible combinations of model values [15]. We feel that it is almost impossible to see the problem as this type of black-box function with more than two inputs. Instead, it is better to have an integrated model of oxygenation, titration and carbamination.

Today, allosteric hemoglobin oxygenation models do exist that seem more in agreement with the structural knowledge of hemoglobin [12, 46-48]. These models take into account two or more structurally different forms: relaxed and tensed. However, these models have so far been limited to hemoglobin oxygenation only. Our Adair-based model can explain not only oxygen and carbon dioxide saturation, but also their cooperation with acid-base buffering properties of hemoglobin. All three of these connected phenomena fit to measured data in physiological ranges. The limitation of our model is that it does not contain the tetramer space conformations. In future the model could be extended with dependences on electrolytes such as chloride, 2,3-bisphosphoglycerate or other organic phosphates and their binding reactions, as many research studies show these interactions [49-52]. The oxygenation could also be improved for the allosteric models [12, 48], assuming that oxy-reactions are almost in relaxed forms and deoxy-reactions are in tensed forms. The next extension of this model could be performed by the integration of an intracellular red cell environment to calculate with phosphate acid-base buffers, and finally the membrane changes with blood plasma, where the chloride shift reaches a Gibbs-Donnan equilibrium and establishes chloride, bicarbonate and hydrogen ion activity ratios. Having an integrated model of blood gases and acid-base is crucial if we want the precise computational algorithms of the current state of a patient. These calculations could be used, for example, inside the next generation of medical devices to estimate not only blood properties, but also the connected properties of circulation [38] or metabolic functions [40].

In this article, we present a hemoglobin model that integrates O_2, CO_2 and H^+ binding. The model is not just empirical, but is based on sound theoretical principles, such as the competitive binding of CO_2 and H+ on the valine-1 NH_2 terminus, the Bohr and Haldane effect [9, 53] and on the principle of detailed balance. The principle of detailed balance is used for the first time in the

Adair type of model, offering mass and energy conservation principles, and accumulates substances and heat inside hemoglobin forms, which is very useful for integration in higher-scale dynamic models.

LIST OF ABBREVATIONS

ODC	hemoglobin oxygen dissociation curve
2,3-DPG	2,3-diphosphoglycerate
[X]	molar concentration of X in $mol.m^{-3}$
aH^+	activity of hydrogen ions, where $pH=-\log_{10}(aH^+)$
αO_2	O_2 solubility in $mol.m^{-3}.Pa^{-1}$
αCO_2	CO_2 solubility in $mol.m^{-3}.Pa^{-1}$
pO_2	partial pressure of O_2 in Pa
pCO_2	partial pressure of CO_2 in Pa
Hb_u	hemoglobin alpha or beta subunit
Hb_{uD}	deoxygenated Hb_u
Hb_{uO}	oxygenated Hb_u
$Hb_uNH_3^+$	Hb_u with protonated N-terminus
$Hb_{uD}NH_3^+$	Hb_{uD} with protonated N-terminus
$Hb_{uO}NH_3^+$	Hb_{uO} with protonated N-terminus
Hb_uNH_2	Hb_u with $–NH_2$ form of N-terminus
$Hb_{uD}NH_2$	Hb_{uD} with $–NH_2$ form of N-terminus
$Hb_{uO}NH_2$	Hb_{uO} with $–NH_2$ form of N-terminus
Hb_uCOO^-	Hb_u with carboxylated N-terminus
$Hb_{uD}COO^-$	Hb_{uD} with carboxylated N-terminus
$Hb_{uO}COO^-$	Hb_{uO} with carboxylated N-terminus
Hb_uAH	Hb_u with protonated side-chains
$Hb_{uD}AH$	Hb_{uD} with protonated side-chains
$Hb_{uO}AH$	Hb_{uO} with protonated side-chains
Hb_uA^-	Hb_u with deprotonated side-chains
$Hb_{uD}A^-$	Hb_{uD} with deprotonated side-chains
$Hb_{uO}A^-$	Hb_{uO} with deprotonated side-chains
$Hb_uA^-NH_2$	selected normalized form of Hb_u with deprotonated side-chains and $-NH_2$ form of N-terminus
$Hb_{uD}A^-NH_2$	deoxygenated form of $Hb_uA^-NH_2$
$Hb_{uO}A^-NH_2$	oxygenated form of $Hb_uA^-NH_2$
f_{nD}	fraction of $Hb_{uD}A^-NH_2$ from Hb_{uD}
f_{nO}	fraction of $Hb_{uO}A^-NH_2$ from Hb_{uO}
f_{zcD}	fraction of $Hb_{uD}NH_2$ form Hb_{uD}
f_{zcO}	fraction of $Hb_{uO}NH_2$ form Hb_{uO}
f_{hD}	fraction of $Hb_{uD}A^-$ form Hb_{uD}
f_{hO}	fraction of $Hb_{uO}A^-$ form Hb_{uO}
ΔH_h^+	change of valence (charge) on side-chains during deoxygenation per one Hb_u
ΔH_z^+	protonation of $–NH_2$ form of N-terminus during deoxygenation per one Hb_u
ΔH_c^+	decarboxylation of carboxylated N-terminus during deoxygenation per one Hb_u
ΔH^+	Haldane coefficient per hemoglobin subunit
Hb_t	hemoglobin tetramer without bound O_2 molecules
$(O_2)_iHb_t$	hemoglobin tetramer with the number of *i* bound O_2 molecules

$(O_2)_iHb_{tn}$	hemoglobin tetramer composed only of $Hb_uA^-NH_2$ subunit forms with the number of *i* bound O_2 molecules
sO_2	O_2 saturation of hemoglobin
sCO_{2D}	CO_2 saturation of deoxyhemoglobin
sCO_{2O}	CO_2 saturation of oxyhemoglobin
sCO_2	CO_2 saturation of hemoglobin
tCO_2	total concentration of CO_2 = free dissolved CO_2 + HCO_3^- + CO_3^{2-} + Hb_uCOO^-
dTH	shift of titration curve, which equals how many mols of titrant must be added to one mol of hemoglobin subunit to reach the same pH of the base (O_2- and CO_2-free) titration curve
pH	acidity/basicity of hemoglobin solution (e.g. inside erythrocytes)
pH_p	pH in plasma (e.g. acidity/basicity of blood)

ACKNOWLEDGMENTS

This work was supported by grants from the Ministry of Industry and Trade of the Czech Republic: MPO TIP TI3/869 – Virtual patient for medical education; and by The Ministry of Education, Youth and Sports via the grant SVV-2014-260033. In addition, the main author wants to thank doc. MUDr. Jiří Kofránek, CSc. and Prof. MUDr. Emanuel Nečas, DrSc. for critical review and Austin Schaefer for English language editing.

REFERENCES

[1] Matthew JB, Morrow J, Wittebort RJ, Gurd F. Quantitative determination of carbamino adducts of alpha and beta chains in human adult hemoglobin in presence and absence of carbon monoxide and 2, 3-diphosphoglycerate. J Biol Chem 1977;252:2234-44.
[2] Perutz M. Species adaptation in a protein molecule. Mol Biol Evol 1983;1:1-28.
[3] Perutz M, Kilmartin J, Nishikura K, Fogg J, Butler P, Rollema H. Identification of residues contributing to the Bohr effect of human haemoglobin. J Mol Biol 1980;138:649-68.
[4] Rossi-Bernardi L, Roughton F. The specific influence of carbon dioxide and carbamate compounds on the buffer power and Bohr effects in human haemoglobin solutions. J Physiol 1967;189:1-29.
[5] Forster R, Constantine H, Craw MR, Rotman H, Klocke R. Reaction of CO2 with human hemoglobin solution. J Biol Chem 1968;243:3317-26.
[6] Stadie WC, O'Brien H. The carbamate equilibrium I. The equilibrium of amino acids, carbon dioxide, and carbamates in aqueous solution; with a note on the Ferguson-Roughton carbamate method. J Biol Chem 1936;112:723-58.
[7] Morrow J, Matthew J, Wittebort R, Gurd F. Carbon 13 resonances of 13CO2 carbamino adducts of alpha and beta chains in human adult hemoglobin. J Biol Chem 1976;251:477-84.
[8] Bohr C, Hasselbalch K, Krogh A. Ueber einen in biologischer Beziehung wichtigen Einfluss, den die Kohlensäurespannung des Blutes auf dessen Sauerstoffbindung übt. Skandinavisches Archiv für Physiologie 1904;16:402-12.
[9] Siggaard-Andersen O, Garby L. The Bohr effect and the Haldane effect. Scand J Clin Lab Invest 1973;31:1-8.
[10] Tyuma I. The Bohr effect and the Haldane effect in human hemoglobin. Jpn J Physiol 1984;34:205.

[11] Matthew J, Hanania G, Gurd F. Electrostatic effects in hemoglobin: hydrogen ion equilibria in human deoxy-and oxyhemoglobin A. Biochemistry 1979;18:1919.
[12] Monod J, Wyman J, Changeux J-P. On the nature of allosteric transitions: a plausible model. J Mol Biol 1965;12:88-118.
[13] Eaton WA, Henry ER, Hofrichter J, Bettati S, Viappiani C, Mozzarelli A. Evolution of allosteric models for hemoglobin. IUBMB Life 2007;59:586-99.
[14] Hill AV. The combinations of haemoglobin with oxygen and with carbon monoxide. I. Biochem J 1913;7:471.
[15] Siggaard-Andersen O, Siggaard-Andersen M. The oxygen status algorithm: a computer program for calculating and displaying pH and blood gas data. Scand J Clin Lab Invest 1990;50:29-45.
[16] Adair GS. The hemoglobin system VI. The oxygen dissociation curve of hemoglobin. J Biol Chem 1925;63:529-45.
[17] Dash RK, Bassingthwaighte JB. Erratum to: Blood HbO2 and HbCO2 dissociation curves at varied O2, CO2, pH, 2, 3-DPG and temperature levels. Ann Biomed Eng 2010;38:1683-701.
[18] Severinghaus JW. Simple, accurate equations for human blood O2 dissociation computations. J Appl Physiol 1979;46:599-602.
[19] Christiansen J, Douglas C, Haldane J. The absorption and dissociation of carbon dioxide by human blood. J Physiol 1914;48:244-71.
[20] Perrella M, Bresciani D, Rossi-Bernardi L. The binding of CO2 to human hemoglobin. J Biol Chem 1975;250:5413-8.
[21] Mateják M, Kulhánek T, Šilar J, Privitzer P, Ježek F, Kofránek J. Physiolibrary-Modelica library for Physiology. 10th International Modelica Conference; 2014 March 12; Lund, Sweden: Linköping University Electronic Press; 2014. p. 499-505.
[22] Mateják M. Physiology in Modelica. Mefanet J 2014;2:10-4.
[23] Siggaard-Andersen O. Oxygen-Linked Hydrogen Ion Binding of Human Hemoglobin. Effects of Carbon Dioxide and 2, 3-Diphosphoglycerate I. Studies on Erythrolysate. Scand J Clin Lab Invest 1971;27:351-60.
[24] Bauer C, Schröder E. Carbamino compounds of haemoglobin in human adult and foetal blood. J Physiol 1972;227:457-71.
[25] Reeves RB. The effect of temperature on the oxygen equilibrium curve of human blood. Respir Physiol 1980;42:317-28.
[26] Kulhanek T, Matejak M, Silar J, Kofranek J. Parameter estimation of complex mathematical models of human physiology using remote simulation distributed in scientific cloud. Biomedical and Health Informatics (BHI), 2014 IEEE-EMBS International Conference on; 2014 1-4 June 2014; 2014. p. 712-5.
[27] Sendroy J, Dillon RT, Van Slyke DD. Studies of gas and electrolyte equilibria in blood XIX. The solubility and physical state of uncombined oxygen in blood. J Biol Chem 1934;105:597-632.
[28] Maas A, Rispens P, Siggaard-Andersen O, Zijlstra W. On the reliability of the Henderson-Hasselbalch equation in routine clinical acid-base chemistry. Ann Clin Biochem 1984;21:26.
[29] Antonini E, Wyman J, Brunori M, Fronticelli C, Bucci E, Rossi-Fanelli A. Studies on the relations between molecular and functional properties of hemoglobin V. The influence of temperature on the Bohr effect in human and in horse hemoglobin. J Biol Chem 1965;240:1096-103.
[30] Sauro HM. Enzyme Kinetics for Systems Biology. Future Skill Software; 2011. p. 20-1.

[31] Naeraa N, Petersen ES, Boye E. The influence of simultaneous, independent changes in pH and carbon dioxide tension on the in vitro oxygen tension-saturation relationship of human blood. Scand J Clin Lab Invest 1963;15:141-51.
[32] Siggaard-Andersen O, Salling N. Oxygen-linked hydrogen ion binding of human hemoglobin. Effects of carbon dioxide and 2, 3-diphosphoglycerate. II. Studies on whole blood. Scand J Clin Lab Invest 1971;27:361-6.
[33] Lide DR. CRC handbook of chemistry and physics: CRC press; 2004.
[34] Atha DH, Ackers GK. Calorimetric determination of the heat of oxygenation of human hemoglobin as a function of pH and the extent of reaction. Biochemistry 1974;13:2376-82.
[35] Siggaard-Andersen O. Acid-base balance. Encyclopedia of respiratory medicine 2005:1-6.
[36] Hester RL, Brown AJ, Husband L, Iliescu R, Pruett D, Summers R, Coleman TG. HumMod: a modeling environment for the simulation of integrative human physiology. Front Physiol 2011;2.
[37] Kofranek J, Matousek S, Rusz J, Stodulka P, Privitzer P, Matejak M, Tribula M. The Atlas of Physiology and Pathophysiology: Web-based multimedia enabled interactive simulations. Comput Methods Programs Biomed 2011;104:143-53.
[38] Jarvis SS, Levine BD, Prisk GK, Shykoff BE, Elliott AR, Rosow E, Blomqvist CG, Pawelczyk JA. Simultaneous determination of the accuracy and precision of closed-circuit cardiac output rebreathing techniques. J Appl Physiol 2007;103:867-74.
[39] Sun X-G, Hansen JE, Ting H, Chuang M-L, Stringer WW, Adame D, Wasserman K. Comparison of Exercise Cardiac Output by the Fick Principle Using Oxygen and Carbon Dioxide*. CHEST Journal 2000;118:631-40.
[40] Rees SE, Andreassen S. Mathematical models of oxygen and carbon dioxide storage and transport: the acid-base chemistry of blood. Crit Rev Biomed Eng 2005;33.
[41] Imai K, Yonetani T. PH dependence of the Adair constants of human hemoglobin. Nonuniform contribution of successive oxygen bindings to the alkaline Bohr effect. J Biol Chem 1975;250:2227-31.
[42] Adair G, Cordero N, Shen T. The effect of temperature on the equilibrium of carbon dioxide and blood and the heat of ionization of haemoglobin. The Journal of physiology 1929;67:288-98.
[43] Chipperfield J, Rossi-Bernardi L, Roughton F. Direct calorimetric studies on the heats of ionization of oxygenated and deoxygenated hemoglobin. J Biol Chem 1967;242:777-83.
[44] Weber RE, Campbell KL. Temperature dependence of haemoglobin–oxygen affinity in heterothermic vertebrates: mechanisms and biological significance. Acta Physiologica 2011;202:549-62.
[45] Weber RE, Fago A, Campbell KL. Enthalpic partitioning of the reduced temperature sensitivity of O2 binding in bovine hemoglobin. Comparative Biochemistry and Physiology Part A: Molecular & Integrative Physiology 2014.
[46] Szabo A, Karplus M. A mathematical model for structure-function relations in hemoglobin. J Mol Biol 1972;72:163-97.
[47] Brunori M, Coletta M, Di Cera E. A cooperative model for ligand binding to biological macromolecules as applied to oxygen carriers. Biophys Chem 1986;23:215-22.
[48] Henry ER, Bettati S, Hofrichter J, Eaton WA. A tertiary two-state allosteric model for hemoglobin. Biophys Chem 2002;98:149-64.
[49] de Bruin SH, Rollema HS, Janssen LH, van Os GA. The interaction of chloride ions with human hemoglobin. Biochem Biophys Res Commun 1974;58:210-5.

[50] Rollema HS, de Bruin SH, Janssen L, Van Os G. The effect of potassium chloride on the Bohr effect of human hemoglobin. J Biol Chem 1975;250:1333-9.
[51] Benesch R, Benesch RE, Yu CI. Reciprocal binding of oxygen and diphosphoglycerate by human hemoglobin. Proc Natl Acad Sci U S A 1968;59:526.
[52] Bunn HF, Briehl RW. The interaction of 2, 3-diphosphoglycerate with various human hemoglobins. J Clin Invest 1970;49:1088.
[53] Siggaard-Andersen O, Salling N, Nörgaard-Pedersen B, Rørth M. Oxygen-Linked Hydrogen Ion Binding of Human Hemoglobin. Effects of Carbon Dioxide and 2, 3-Diphosphoglycerate: III. Comparison of the Bohr Effect and the Haldane Effect. Scand J Clin Lab Invest 1972;29:185-93.